Macromolecules 1982, *15*, 762–770

Effects of Annealing and Prior History on Enthalpy Relaxation in Glassy Polymers. 2. Mathematical Modeling

Ian M. Hodge* and Alan R. Berens

BFGoodrich Research and Development Center, Brecksville, Ohio 44141.
Received August 24, 1981

ABSTRACT: A simple four-parameter model reproduces DSC data on the effects of annealing conditions, and thermal history before annealing, on the heat capacity of glassy polymers. The model is an application of the successful treatment of glass transition kinetics, due to Moynihan and co-workers, to thermal histories which include annealing. It is found that a nonexponential relaxation function is essential for the development of sub-T_g heat capacity peaks with annealing and that nonlinearity is important in accelerating their development to experimentally accessible aging times. Numerical integration allows accurate predictions of the effects of quench rate, annealing temperature, annealing time, and reheating rate on the magnitude and temperature of heat capacity peaks observed in DSC scans of annealed PVC (part 1) and other polymeric glasses.

I. Introduction

Glasses usually exist in a nonequilibrium state, and relaxation toward equilibrium is commonly referred to as physical aging or annealing. Aging affects a large number of properties such as density, modulus, and the rate of stress, strain, enthalpy, and volume relaxation.[1-3]

The increased rate of aging as temperature approaches the glass transition temperature, T_g, and the elimination of aging effects after heating above T_g suggest a close connection between the aging and glass transition phenomena. Furthermore, Kovacs et al.[2,3] and the present authors[4] have demonstrated that the development of sub-T_g heat capacity peaks with aging is a consequence of the glass transition kinetics. The present paper explores in detail the relation between the glass transition phenomenon and aging effects. The approach used by Moynihan and co-workers[5] to treat the glass transition is used to calculate the heat capacity as a function of glass transition kinetic parameters, annealing conditions, and thermal history before annealing. A comparison with experimental data given in part 1 is also made. We begin by reviewing some of the phenomenological aspects of the glass transition kinetics, as treated by Moynihan and coworkers.[5]

The kinetics of the glass transition and aging phenomena are both nonexponential and nonlinear. They are nonexponential in the sense that the relaxation toward equilibrium following a sudden perturbation (e.g., a temperature step) is described by a nonexponential decay function $\phi(t)$. This is formally equivalent to a distribution of relaxation times $g(\tau)$, related to $\phi(t)$ by

$$\phi(t) = \int_0^\infty g(\tau) e^{-t/\tau}\, d\tau \tag{1}$$

and constrained by the condition

$$\int_0^\infty g(\tau)\, d\tau = 1 \tag{2}$$

The description of a relaxation by a specific function for $g(\tau)$ does not necessarily imply separate relaxation mechanisms for the various relaxation time components of $g(\tau)$, since a single cooperative relaxation mechanism may produce a nonexponential form for $\phi(t)$. A well-known consequence of a nonexponential relaxation is the maximum in the response (e.g., volume) to two separate perturbations of opposite sign (e.g., temperature jumps).[3,5] An empirical function which has been found to give an excellent fit to a wide range of relaxation processes in a large variety of amorphous materials is

$$\phi(t) = \exp[-(t/\tau_0)^\beta] \tag{3}$$

where τ_0 is a characteristic time and β ($0 < \beta \leq 1$) is a direct measure of nonexponentiality. The corresponding $g(\tau)$ is asymmetric on a log τ scale, with a skew toward short times.[6] Plots of eq 3 are shown in Figure 1 for β = 1.0 (single relaxation time) and β = 0.5 (a representative value). Compared with the exponential function, $\phi(t)$ for β = 0.5 has both shorter and longer time components. This has important consequences for aging behavior which are discussed below. In this paper we shall accept eq 3 as an adequate description of the nonexponentiality of the glass transition and use it to model aging.

The kinetics of aging and the glass transition are also nonlinear in the sense that $\phi(t)$ depends on the degree of departure from equilibrium. This nonlinearity is most conveniently treated by making the average relaxation time a function of structure as well as temperature. It is an additional convenience to treat the structural state of a system, as measured by macroscopic properties such as volume or enthalpy, in terms of the fictive temperature T_f.[7] In the general case, T_f is defined as the temperature at which the measured value of a property would be the equilibrium one. However, since T_f measures only the relaxational component of a specified property, values of T_f assessed from different properties for the same glass may differ. The equilibrium state well above T_g is characterized by the condition $T_f = T$, and relaxation from a nonequilibrium state is described by the decay of T_f toward T. Nonlinearity is treated phenomenologically by allowing τ_0 in eq 3 to be an explicit function of T and T_f, as in the expression of Gardon and Narayanaswamy[8,9]

$$\tau_0 = A \exp\left[\frac{x\Delta h^*}{RT} + \frac{(1-x)\Delta h^*}{RT_f}\right] \tag{4}$$

where A, x ($0 < x \leq 1$), and Δh^* are constants and R is the ideal gas constant. The parameter x is a direct measure of nonlinearity, with $x = 1$ for a linear relaxation. Equations 3 and 4 accurately describe both the decay of refractive index n in response to a single temperature jump and the maximum in n following two large temperature jumps of opposite sign for glassy B_2O_3.[5] The relaxation of enthalpy H following a large temperature jump (20 K) is also accurately described by eq 3 and 4 for the chalcogenide glass As_2Se_3.[5]

Combination of eq 3 and 4 with the Boltzmann superposition principle (as described below) has been used by Moynihan and co-workers[5,10-12] to give an accurate description of the heat capacity C_p as a function of temperature during rate cooling and reheating through the

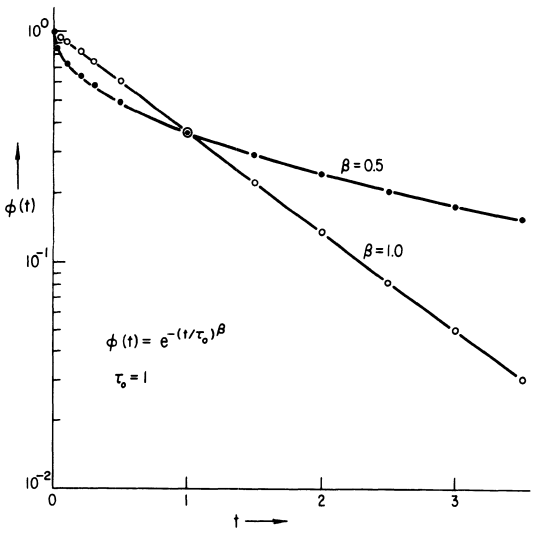

Figure 1. Plots of the decay function given by eq 3 for $\beta = 1.0$ and $\beta = 0.5$.

glass transition for a variety of glasses, including B_2O_3,[10] As_2Se_3,[10] $NaKSi_3O_7$,[11] "5-phenyl-4-ether" [$C_6H_5(OC_6H_4)_3$-OC_6H_5],[5] and poly(vinyl acetate) (PVAc).[12] In particular, the C_p overshoot near T_g during reheating after rate cooling as a function of cooling and heating rates is accurately described.

The development of sub-T_g heat capacity peaks with aging has been well established experimentally since the pioneering work of Illers[15] (see part 1 for further references). We describe here a procedure for accurately calculating these peaks.

II. Model

We first give a summary of the relevant features of Moynihan's treatment of the glass transition kinetics[5,10] and then describe how annealing is introduced.

The glass transition is treated as a straightforward application of the Boltzmann superposition principle of aftereffects, with the nonexponentiality and nonlinearity described by eq 3 and 4, respectively. For heating or cooling rate Q, the time t and temperature T variables are simply related as

$$dT = Q\,dt \tag{5}$$

so that the Boltzmann superposition integral over time can be replaced by a corresponding integral over temperature. Thus the response $T_f(T)$ to temperature perturbations is given by

$$T_f(T) = T_0 + \int_{T_0}^{T} dT' \left\{1 - \exp\left[-\left(\int_{T'}^{T} dT''/Q\tau_0\right)^\beta\right]\right\} \tag{6}$$

where T_0 is a starting temperature well above T_g, and T' and T'' are dummy temperature variables. The value of τ_0 varies continuously with T and T_f according to eq 4. A dimensionless heat capacity $C_p(T)$ is defined as

$$C_p(T) = dT_f/dT \tag{7}$$

and is calculated by differentiating eq 6 during cooling from T_0 to a temperature far below T_g and reheating to T_0 again. The relation between $C_p(T)$ and experimental data is described below. The calculated heat capacity during heating, corresponding to the usual DSC scans, therefore depends on both the heating rate and the previous cooling rate through T_g. Equations 4 and 6 comprise the model for the glass transition phenomenon. The present model for annealing is obtained by inserting the annealing time into the cooling cycle at the annealing temperature in the manner described below.

III. Method of Computation

In practice, eq 6 must be integrated numerically. For this purpose continuous cooling or reheating at a rate Q is replaced by a series of temperature steps, ΔT, followed by isothermal holds of duration $\Delta t = \Delta T/Q$. The magnitude of ΔT must be sufficiently small to ensure linearity; $\Delta T = 1$ K is satisfactory[10] and was used for all the calculations reported here. The evolution of T_f following n temperature steps is then expressed by rewriting eq 6 in the form

$$T_{f,n} = T_0 + \sum_{j=1}^{n} \Delta T_j \{1 - \exp[-(\sum_{k=j}^{n} \Delta T_k/Q_k\tau_{0,k})^\beta]\} \tag{8}$$

where $\tau_{0,k}$ is given by

$$\tau_{0,k} = A \exp\left[\frac{x\Delta h^*}{RT_k} + \frac{(1-x)\Delta h^*}{RT_{f,k-1}}\right] \tag{9}$$

The heat capacity corresponding to eq 7 is given by

$$C_{p,n} = \frac{dT_f}{dT} = \frac{T_{f,n} - T_{f,n-1}}{T_n - T_{n-1}} \tag{10}$$

In fitting the model to experimental data, one must normalize the latter by extrapolating the experimental glass and rubber heat capacities into the glass transition region and expressing the measured heat capacities in excess of C_p(glass) as a fraction of the difference C_p(rubber) – C_p(glass). This normalized C_p has a value zero for the glass and unity for the liquid and is directly comparable with the calculated $C_p(T)$ given by eq 10.

Aging at temperature T_k is introduced into the calculation, in essence, by replacing the term $\Delta T_k/Q_k$ in eq 8 with the annealing time t_e. In the preliminary communication of this model,[4] t_e was inserted directly into eq 8 in this way during the cooling cycle. The calculation proceeded by cooling at a rate Q_C to the aging temperature T_e, holding at that temperature for time t_e, cooling at the same rate to room temperature (300 K), and reheating immediately at heating rate Q_H. The relaxation time τ_0 of eq 3 was assumed constant over the time t_e; i.e., no account was made of the self-retarding (nonlinear) aging kinetics. Although this approximation is sufficiently good to permit the prediction of general changes in the heat capacity maximum ($C_{p\,max}$) and the temperature at which it occurs (T_{max}) with t_e and T_e for PVC,[4] it was necessary to make the parameter x increase explicitly with T_e to give a quantitative account of the experimental data. This shortcoming is largely removed in the computation procedure described here, which incorporates the self-retarding kinetics of aging. The present calculation fits experimental data reasonably well with a single set of four parameters (two of which are constrained by the value of T_g and its variation with quench rate). The self-retarding kinetics were introduced by dividing the aging time into 10 subintervals and calculating T_f and τ_0 at the end of each. Because of the well-established dependence of aging effects on log t_e, the subintervals were determined by dividing t_e into even logarithmically spaced intervals.

During annealing, T is, of course, held constant so that $Q_C = 0$, and eq 8 must be modified to prevent a singularity in the summation over k. This was done by truncating the sum over j in eq 8, with the maximum value of j held fixed at the value at the beginning of the annealing time ($j = n_A$). The summation over k was not truncated, the max-

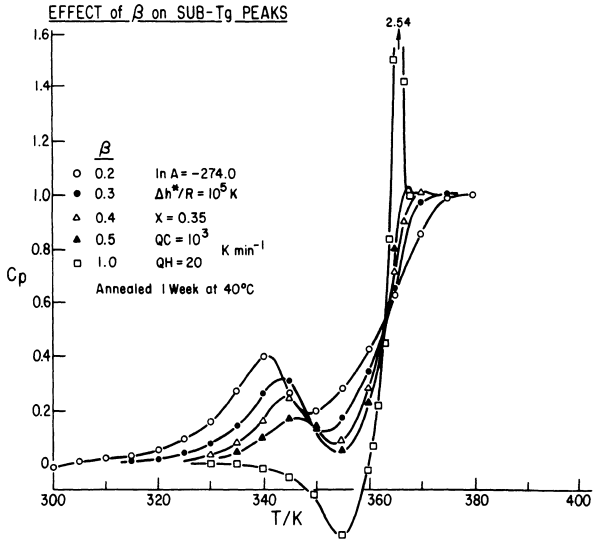

Figure 2. Calculated effect of the nonexponentiality parameter β (eq 3) on the development of sub-T_g heat capacity peaks after annealing at 40 °C for 1 week.

imum value of k being incremented for each subinterval of the aging time. Thus, during annealing eq 8 was modified to

$$T_{f,n} = T_0 + \sum_{j=1}^{n_A} \Delta T_j \{1 - \exp[-(\sum_{k=n_A}^{n} \Delta t_{e,k}/\tau_{0,k})^{\beta}]\} \quad (11)$$

where $n_A + 10 \geq n > n_A$ and

$$\Delta t_{e,k} = t_e^{1/10} \qquad k = n_A + 1$$

$$\Delta t_{e,k} = t_e^{(k-n_A)/10} - t_e^{(k-n_A-1)/10} \qquad k > n_A + 1$$

Equation 11 is a summation version of the integral expressions of Moynihan et al.[5,10] At the first temperature step after annealing, the upper limit of j was increased from n_A to $n_A + 11$ and the summation over j recommenced using eq 8. As before,[4] annealing was introduced during the cooling cycle. This is clearly an approximation to most experimental thermal histories, but since these are rarely specified exactly the precise difference is not known.

IV. Calculation Results

We present the model predictions in three sections. In the first, the effects of varying the model parameters are investigated, with the annealing conditions and other aspects of the thermal history held constant. In the second, the model parameters are held fixed and the predicted effects of changes in annealing conditions and thermal history (such as cooling rate before annealing) are presented. In the Discussion the model predictions are compared with experimental data, some of which were presented in part 1. Some additional results of special interest are also given in the Discussion.

The results presented here are the calculated C_p curves for the reheating cycle, corresponding to the experimental DSC scans. In most cases the value of T_g was fixed at 363 K, close to that of PVC. For this purpose, T_g is defined as the temperature at which the normalized C_p is 0.5 during heating at 20 K min^{-1} after cooling at 10^3 K min^{-1}.

A. Variation of Model Parameters. Variations in the nonexponentiality parameter β (eq 3), nonlinearity parameter x (eq 4), activation enthalpy Δh^* (eq 4), and preexponential factor A (eq 4) were studied. The parameters β and x were each varied individually, with the other three held fixed, and Δh^* and A were varied together to keep T_g constant at 363 K. To assess the importance of the relative difference between T_e and T_g, the parameter A was also varied alone to change T_g.

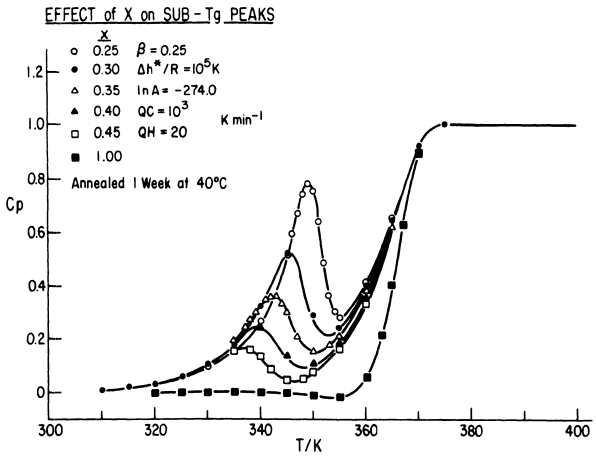

Figure 3. Calculated effect of the nonlinearity parameter x (eq 4) on the development of sub-T_g heat capacity peaks after annealing at 40 °C for 1 week.

1. Nonexponentiality Parameter β. The dimensionless parameter β is a direct measure of nonexponentiality or, equivalently, the breadth of the distribution of relaxation times. Smaller values of β correspond to increased nonexponentiality. Typically, β lies in the range 0.4–0.6 for the glass transition.[5] The calculated effects of changing β on C_p during reheating of an aged glass are shown in Figure 2. The other parameters were fixed at $\Delta h^*/R = 1.0 \times 10^5$ K, $A = 1.01 \times 10^{-119}$ s, and $x = 0.35$, and the experimental variables were fixed at $T_e = 40$ °C, $t_e = 1$ week, $Q_C = 10^3$ K min^{-1}, and $Q_H = 20$ K min^{-1}. Note that A is an empirical parameter with no direct physical significance. The value of Q_C is an estimate of the rate usually referred to in the literature as a "rapid quench". Figure 2 demonstrates that a distinct sub-T_g heat capacity peak is predicted to occur when $\beta < 1$ but not when $\beta = 1.0$. The peaks are asymmetric, with a low-temperature tail and relatively sharp high-temperature edge. This asymmetry is observed experimentally (e.g., see part 1). The results shown in Figure 2 also indicate that T_{max} decreases and $C_{p\,max}$ increases with decreasing β, and this trend continues for values of β between 0.5 and 1.0 (not shown). The limiting case of $\beta = 1.0$ is considered in the Discussion. The glass transition broadens with decreasing β, as expected, but T_g ($C_p = 0.5$) is unaffected.

2. Nonlinearity Parameter x. The effects of changing x on the calculated C_p scans are shown in Figure 3. The other model parameters and the experimental variables are given in the figure. The calculations indicate that both T_{max} and $C_{p\,max}$ increase with decreasing x (increasing nonlinearity). The effect on $C_{p\,max}$ is the same as, and that on T_{max} the opposite of, decreasing β. This difference in response to variations in x and β permits an unambiguous choice of these parameters when fitting the model to experimental data. Indeed, the calculations performed to date suggest that the development of C_p peaks with annealing is more sensitive to x and β than are the shape of the glass transition and the overshoot behavior at T_g as a function of relative cooling and reheating rates. The limiting case of $x = 1$, where $C_{p\,max} = 0$, is considered in the Discussion.

3. Activation Enthalpy Δh^*. The parameter Δh^* (eq 4) can be obtained from the dependence of the frozen-in fictive temperature, T_f', on cooling rate[10] and is not considered as adjustable in the analysis of the kinetics of the glass transition.[10] However, for the purposes of illustrating how annealing behavior is affected by Δh^*, we shall regard

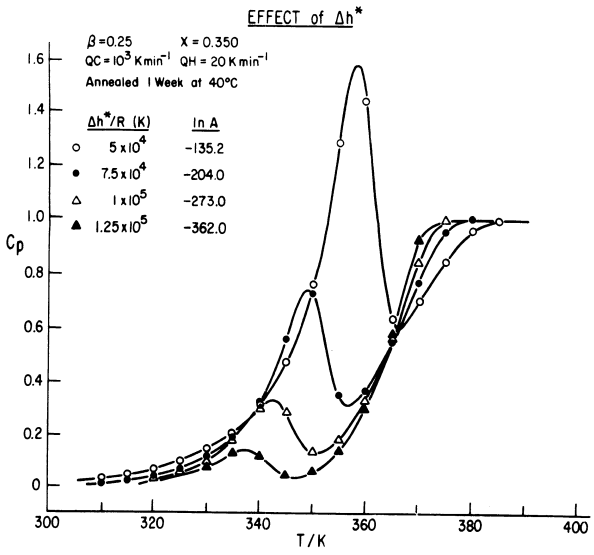

Figure 4. Calculated effect of the parameter Δh^* (eq 4) on the development of sub-T_g heat capacity peaks after annealing at 40 °C for 1 week.

Table I
Calculated Effect of T_g on Development of Sub-T_g C_p Endotherms[a]

T_g, K	T_e, K	$C_{p\,max}$	T_{max}, K
353	313	0.66	341
	323	1.41	349
	333	2.48	356
363	313	0.35	342
	323	0.77	352
	333	1.56	360
373	313	0.19	343
	323	0.42	354
	333	0.87	363

[a] $\Delta h^*/R = 10^5$ K, $\beta = 0.250$, $x = 0.350$, $Q_C = 10^3$ K min^{-1}, $Q_H = 20$ K min^{-1}, $t_e = 1$ week.

it here as fully adjustable. To keep T_g constant, it is necessary to change the parameter A (eq 4) together with Δh^* (Δh^* and log A are linearly related).

The effects of changing Δh^*, with corresponding changes in A, are displayed in Figure 4. The parameters β and x were kept fixed at 0.25 and 0.35, respectively, and the experimental variables were kept at the values given in IV.A.1. The effect of decreasing Δh^* is qualitatively the same as decreasing x; i.e., both T_{max} and $C_{p\,max}$ increase. This presumably reflects the fact that the product $x\Delta h^*$ determines the temperature dependence of τ_0 when T_f is constant (eq 4).

4. Preexponential Factor A. To determine how the relative values of T_e and T_g affect the development of sub-T_g C_p peaks, A was varied alone to change T_g. The values of $C_{p\,max}$ and T_{max} as a function of T_e and T_g are tabulated in Table I.

The calculated values of $C_{p\,max}$ increase as the difference between T_e and T_g diminishes, regardless of T_g. It is also found that $C_{p\,max}$ is relatively constant when T_g is varied but $T_g - T_e$ is fixed. This is consistent with the qualitative experimental observation that the rate of aging depends on $T_g - T_e$ rather than T_e per se. On the other hand, T_{max} depends principally on T_e, regardless of T_g, provided T_e is sufficiently below T_g (at least for the changes in T_g of up to 20 °C studied here).

B. Variation of Experimental Conditions. The effects of changing experimental variables were calculated with the model parameters fixed at ln $A = -272.0$, $\Delta h^*/R = 10^5$ K, $\beta = 0.25$, and $x = 0.35$. These values are approximately those found to fit PVC data in the simplified preliminary communication.[4] Four variables were varied, one at a time, with the others held fixed: aging time t_e, aging temperature T_e, cooling rate Q_C, and reheating rate Q_H. All of the calculated trends presented here are observed experimentally. A detailed comparison of experimental and calculated results is given in the Discussion.

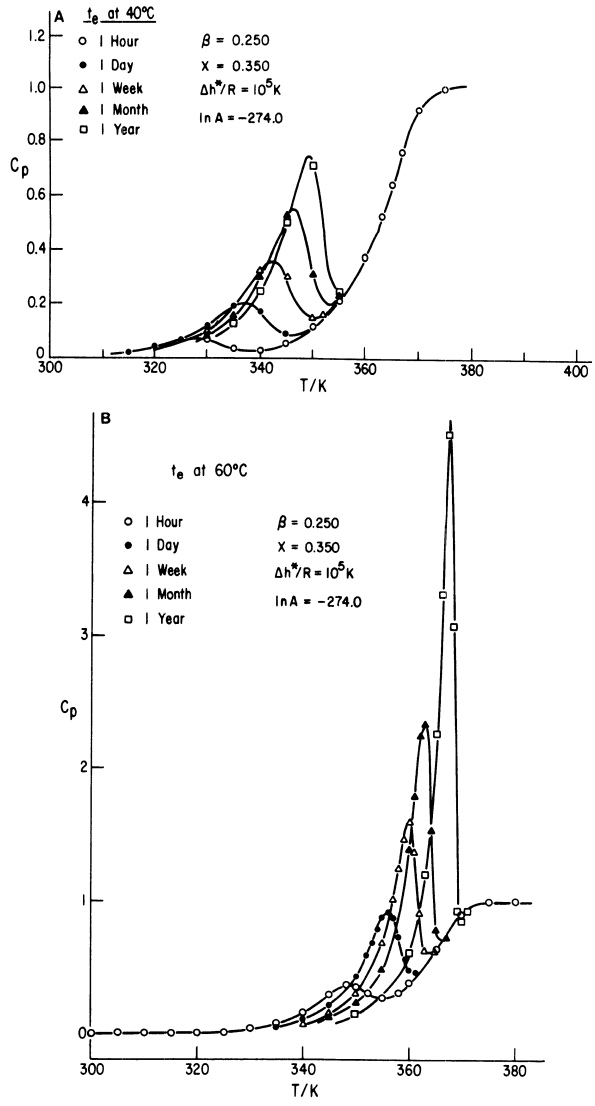

Figure 5. Calculated effect of annealing times from 1 h to 1 year: (A) $T_e = 40$ °C; (B) $T_e = 60$ °C. $Q_C = 10^3$ K min^{-1}, $Q_H = 20$ K min^{-1}.

1. Annealing Time. The effects of aging times from 1 h to 1 year were calculated for aging temperatures of 40 and 60 °C, with the result shown in Figure 5A,B, respectively. It is clear that both T_{max} and $C_{p\,max}$ increase with increasing t_e at both T_e's. When T_{max} lies well below T_g, the glass transition is unaffected by aging, but at the longest t_e's at $T_e = 60$ °C the peak becomes superimposed on the glass transition step and eventually develops into the well-known overshoot. The calculated decrease in T_f during annealing, ΔT_f, is directly comparable with the experimental decrease in enthalpy ΔH. It is calculated that ΔT_f is an approximately linear function of log t_e at short t_e and low T_e (Figure 6A) but becomes independent of t_e at long t_e and high T_e. This leveling off occurs when T_f has relaxed fully to T_e. It is also calculated that T_{max} increases approximately linearly with log t_e (Figure 6B).

2. Annealing Temperature T_e. The effects of annealing temperatures between 30 and 80 °C, calculated at

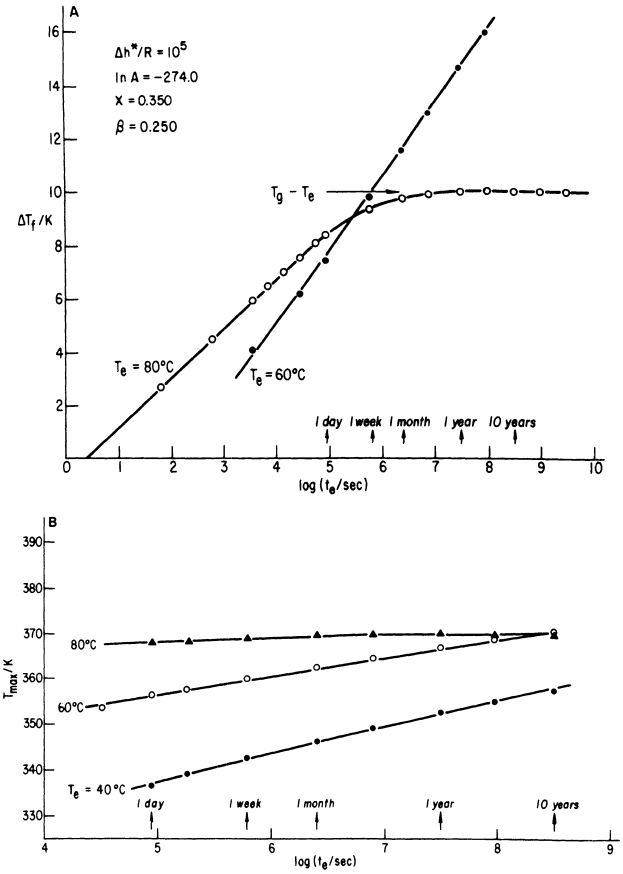

Figure 6. (A) Calculated dependence of ΔT_f on log t_e for T_e = 60 and 80 °C. Here, T_g refers to the value of T_f before annealing. (B) Calculated dependence of T_{max} on log t_e for T_e = 40, 60, and 80 °C. Parameters are given in (A).

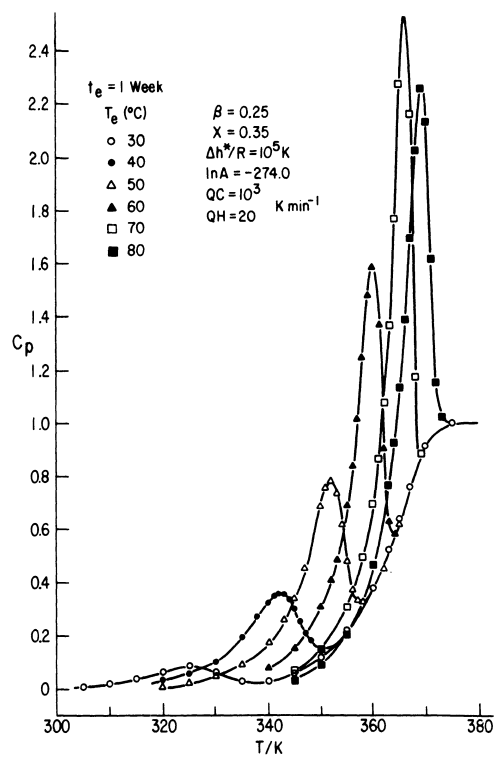

Figure 7. Calculated effects of T_e on C_p for t_e = 1 week.

10 °C intervals for a fixed annealing time of 1 week, are shown in Figure 7. T_{max} increases steadily with T_e, but $C_{p\,max}$ increases only up to T_e = 70 °C and then begins to decrease. When T_e is well below T_g (by ~30 °C or more),

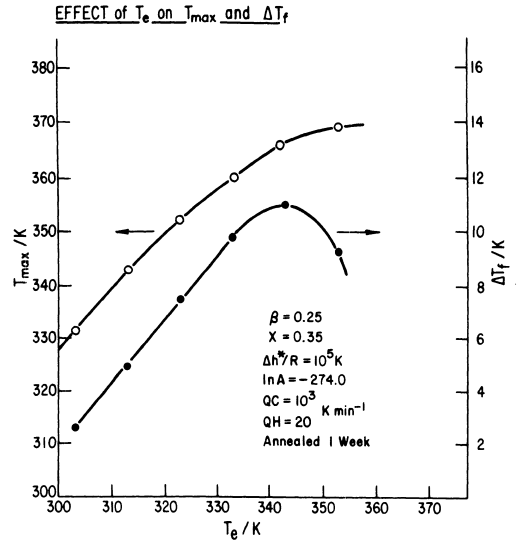

Figure 8. Calculated variation of T_{max} and ΔT_f with T_e for t_e = 1 week.

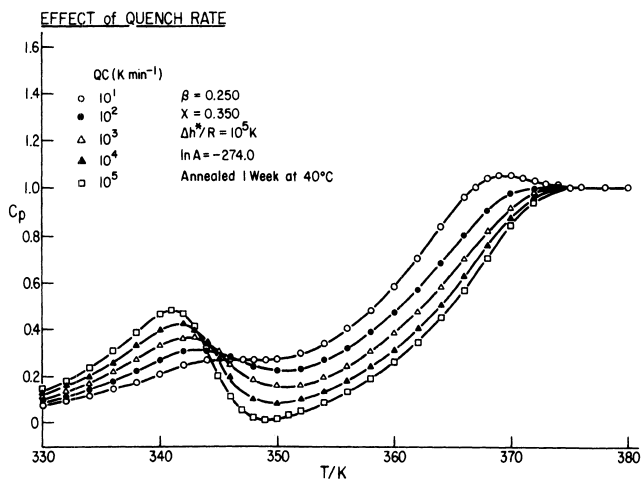

Figure 9. Calculated effects of cooling rate Q_C on the development of C_p peaks with aging. T_e = 40 °C, t_e = 1 week, Q_H = 20 K min^{-1}.

T_{max} is calculated to increase almost linearly with T_e (Figure 8), with curvature occurring at higher values of T_e. The magnitude of ΔT_f also increases linearly with T_e at low T_e and then, like $C_{p\,max}$, passes through a maximum at ca. 70 °C (i.e., 20 °C below T_g) (Figure 8).

3. Cooling Rate. The calculated effects of varying the cooling rate from 10 to 10^5 K min^{-1} at decade intervals before annealing at 40 °C for 1 week are shown in Figure 9. The heating rate is 20 K min^{-1}. It is calculated that $C_{p\,max}$ increases and the peaks become sharper and more asymmetric with increasing quench rate, whereas T_{max} is almost unaffected. At the fastest cooling rate shown in Figure 9 (10^5 K min^{-1}), the minimum in C_p between T_{max} and T_g drops below the unannealed glassy level.

The increase in T_g with increasing quench rate and the overshoot at T_g for the lowest cooling rate are also observed in unannealed glasses.[5,10,28]

4. Reheating Rate. The calculated effects of varying the reheating rates from 10 to 10^3 K min^{-1} at half-decade intervals are shown in Figure 10. The cooling rate was 10^3 K min^{-1}, and annealing for 1 week was introduced at 40 °C. The calculations show that both T_{max} and $C_{p\,max}$ increase with increasing Q_H. Most of the increase in $C_{p\,max}$ with increasing Q_H is due to the rising glass transition background with increasing temperature. T_{max} increases

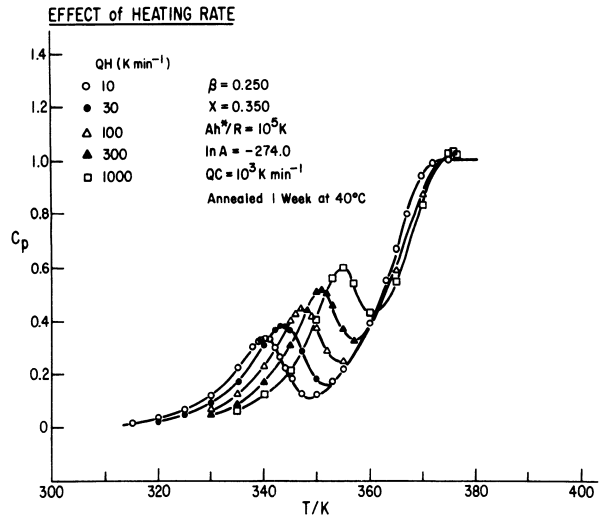

Figure 10. Calculated effects of heating rate on C_p after annealing 1 week at 40 °C.

approximately linearly with log Q_H.

V. Discussion

A. Comparison with Experimental Observations.

1. Effect of Aging Time t_e. The calculated linear increase in T_{max} with log t_e is observed experimentally.[15-17,19,22] The decrease in T_f during annealing, ΔT_f, is directly comparable with the experimental decrease in enthalpy after aging, ΔH, determined from the integrated difference between C_p scans of aged and unaged glasses with otherwise identical thermal histories. For example, a change of 1 K in T_f corresponds to ca. 0.07 cal g^{-1} for PVC. The linear increase in ΔT_f with log t_e at short t_e (Figure 6) is observed experimentally.[3,15,16,18,19] The predicted constancy of ΔT_f at long t_e (Figure 6) is also observed[17,19-21] and is due to T_f relaxing fully to T_e. This corresponds to the experimental situation in which the excess glassy enthalpy relaxes to the equilibrium value.

2. Effect of Annealing Temperature T_e. The calculated linear relation between T_{max} and T_e when T_e is well below T_g (Figure 8) is observed experimentally.[3,15,16,18] The calculated linear relation between ΔT_f and T_e at low T_e (Figure 8) is also observed[15,16,18-20] as is the maximum at 70 °C (ca. 20 °C below T_g).[15,16,20,21,23] This maximum reflects the approach of T_f to T_e after annealing, since the maximum change in T_f is restricted by how much T_f exceeds T_e at the beginning of annealing, and this difference decreases as T_e approaches T_g. For example, at T_e = 80 °C T_f is calculated to exceed T_e by 10 K before annealing and almost all of this (9 K) relaxes out after 1 week of aging. This is much less than the change in T_f of 15 K obtained by extrapolation of the linear region at low T_e.

3. Cooling Rate and Prior History. The calculated increases in peak sharpness, peak asymmetry, and ΔT_f with increasing cooling rate accurately reproduce the experimental data for PVC (see part 1). Similar effects are observed in annealed PVC glasses which were mechanically dilated or swollen by vapor before annealing (part 1) and in annealed PS[17] and PVC[25] glasses which were vitrified under high hydrostatic pressures and annealed at atmospheric pressure. The similarity of the calculated curves to results on pressure-vitrified PVC[25] and PS[17] is particularly striking. These observations suggest that both dilation and densification of glasses elevate their excess enthalpies just as rapid quench rates do.

Another common feature of rapidly quenched, pressure-densified, and mechanically or vapor-dilated glasses is the weak dependence of T_{max} on their prior histories

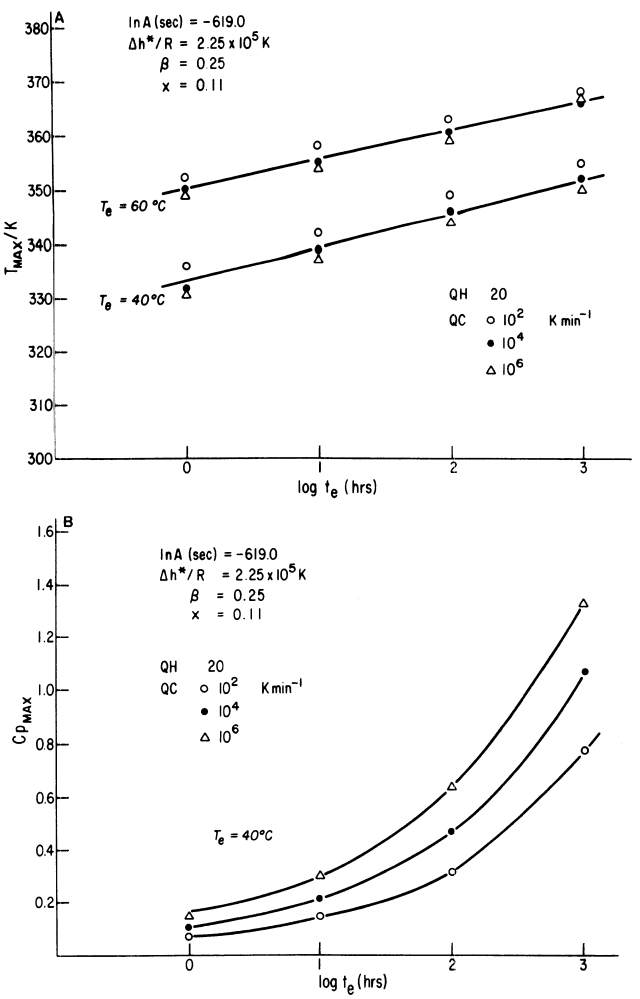

Figure 11. (A) Calculated variation of T_{max} with log t_e as a function of T_e and Q_C. (B) Calculated variation of $C_{p\,max}$ with log t_e at T_e = 40 °C as a function of Q_C (cf. Figure 10 of ref 13).

(Figure 9, part 1). The results presented in IV.B.3 indicate that T_{max} is almost independent of quench rate when the other experimental variables are fixed. The calculation is now extended to include variations in t_e and T_e. The model parameters chosen were those which best fit the experimental data for liquid-nitrogen-quenched PVC (see section V.A.5 below). The calculated effects of varying Q_C and T_e on T_{max} as a function of log t_e are shown in Figure 11A. It is found that T_{max} varies with log t_e in almost the same way for a large range of quench rates and that the slope $(\partial T_{max}/\partial \log t_e)_{T_e}$ is weakly dependent on T_e. These results closely parallel the experimental observations summarized in Figure 9 of part 1. Also, the calculated increase in T_{max} of 6.5 K per decade of t_e is in reasonable agreement with the experimental value of ca. 5 K per decade obtained from Figure 9 of part 1. In contrast to the weak dependence of T_{max} on cooling rate, the values of $C_{p\,max}$ and ΔT_f and their variation with log t_e are quite sensitive to Q_C, as shown in Figure 11B. The more rapid increase in $C_{p\,max}$ with t_e for rapidly quenched glasses reproduces the experimental trends exhibited in Figure 10 of part 1, but the experimental scatter is too large to determine if the calculated curvilinear relation between $C_{p\,max}$ and log t_e is correct.

Yet another feature shared by rapidly quenched, dilated, and densified glasses is the occurrence of exothermic minima. Such exotherms are frequently observed below T_g in glasses which have been rapidly quenched and reheated slowly, and it is now well established that this is

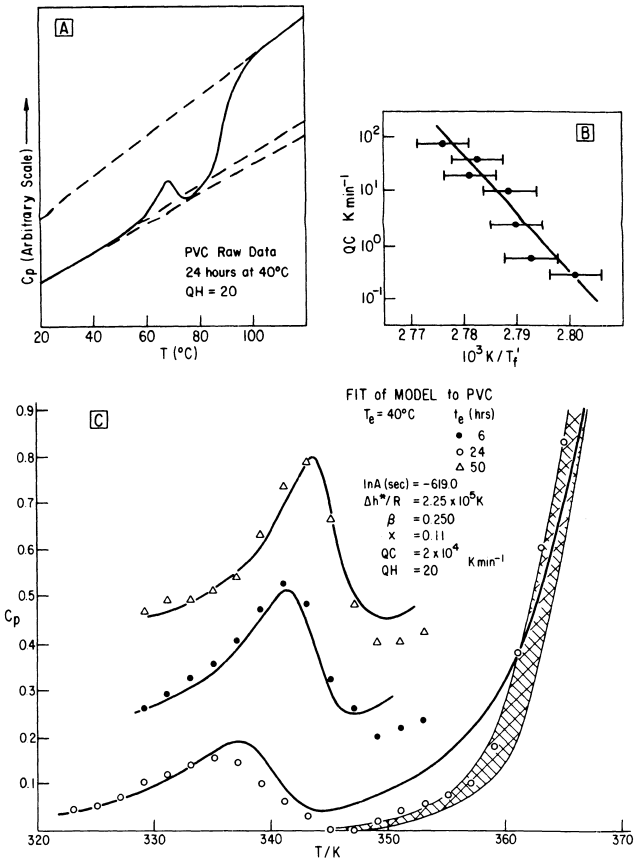

Figure 12. Fit to experimental data for liquid-nitrogen-quenched PVC (from part 1). (A) Representative raw data, with extreme choices for glassy C_p. (B) Dependence of T_f' on Q_C. (C) Experimental data are shown as points, model fits as solid lines. The curves for t_e = 24 and 50 h are displaced upward for clarity, by 0.2 and 0.4, respectively. Crosshatching corresponds to experimental scatter at T_g.

due to partial relaxation of the excess enthalpy to the lower equilibrium enthalpy during slow reheating.[10] The development of a sub-T_g peak with annealing evidently does not significantly change this phenomenon.

The increase in the magnitude of ΔH with increasing quench rate, dilation, or densification is a direct result of the elevated excess enthalpies and the nonlinearity of the relaxation kinetics; the large excess enthalpies reduce the average relaxation time so that aging occurs more rapidly. The increased density of the pressure-densified glasses would also be expected to increase the average volume relaxation time, but any density-induced increase in enthalpy relaxation times is apparently not large enough to reverse the enhanced relaxation rate caused by the large excess enthalpy. An answer to the interesting question of whether changes in density alone affect the enthalpy relaxation rate must await an experimental comparison of enthalpy relaxation in chemically identical glasses with the same excess enthalpies but different densities.

4. Reheating Rate. Only a few systematic studies of the effect of heating rate on sub-T_g C_p peaks have been made.[3,19,26] Analysis of these results indicates that the calculations correctly predict an approximately linear increase in T_{max} with log Q_H. Since the reheating rate affects only the manifestation of enthalpy relaxation during annealing, no change in ΔT_f is expected nor seen.

5. Poly(vinyl chloride) (PVC). Representative data for liquid-nitrogen-quenched PVC, with estimates of C_{p_g} and C_{p_l}, are given in Figure 12A. Two extreme choices of C_{p_g} are shown to illustrate the major source of uncertainty in the normalization procedure. The minimum

Table II
Fit of Model to PVC Data[a]

		$C_{p\,max}$		T_{max}	
T_e, °C	t_e, h	obsd	calcd	obsd	calcd
20	7	0.13	0.08	324	323
	27	0.14	0.12	328	327
	150	0.21	0.21	332	333
40	6	0.16	0.19	336	337
	24	0.33	0.31	341	341
	50	0.40	0.40	343	343
60	1	0.21	0.37	351	350
	7	0.66	0.76	357	355
	24	1.10	1.2	359	357
	50	1.6	1.6	360	359

[a] $\Delta h^*/R = 2.25 \times 10^5$ K, $\beta = 0.250$, $x = 0.110$, ln A = −619.0, $Q_C = 2 \times 10^4$ K min^{-1}, $Q_H = 20$ K min^{-1}.

between T_{max} and T_g is particularly sensitive to this uncertainty. The cooling rate through T_g was estimated as 2×10^4 K min^{-1}, by assuming an exponential decrease in temperature from +120 to −196 °C in 2 s (see part 1). The model parameter Δh^* was determined from separate measurement of T_f' (the value of T_f frozen-in immediately after cooling) as a function of cooling rate in the manner described by Moynihan and co-workers.[5] A plot of log Q_C vs. $1/T_f'$ is given in Figure 12B. The best-fit value for $\Delta h^*/R$ is (2.25 ± 0.25) × 10^5 K. The large imprecision is a result of the estimated uncertainty in T_f (±0.5 K), being large compared with the total change in T_f' of ca. 3 K for a 2 order of magnitude change in Q_C. The parameter A was then fixed by T_g (363 K for the liquid-nitrogen-quenched glass reheated at 20 K min^{-1} when defined as the temperature at which the normalized heat capacity is 0.5). The parameters β and x were varied to give the best overall fit to the data for T_e = 40 °C. Thus, only two parameters were adjusted.

The calculated values of $C_{p\,max}$ and T_{max} as a function of T_e and t_e are compared with experimental data in Table II. In Figure 12C, the experimental and calculated C_p curves for T_e = 40 °C are compared at several t_e's. The band at T_g represents the experimental spread for all the combinations of t_e and T_e listed in Table II.

The agreement between experimental data and model calculations exhibited in Table II and Figure 12C is sufficiently good to be considered as support for the general accuracy of the treatment, especially in view of the experimental uncertainties in quench rate and C_{p_g} and the (unknown) differences in detail of the experimental and modeled thermal histories. In particular, the reproduction of T_{max} and $C_{p\,max}$ for several combinations of t_e and T_e using a single set of four parameters (of which only two were adjusted) is considered strong evidence for the fundamental correctness of the model.

We turn now to a discussion of the parameters. The assumption that Δh^* is independent of temperature is evidently an adequate approximation despite the well-known WLF behavior above T_g. The value of $\Delta h^*/R$ for PVC is much higher than the values obtained by the same method for other glasses.[5] However, it should be recalled that the temperature dependence of the relaxation times at constant T_f is determined by $x\Delta h^*/R$ (eq 4), whose value of 2.5×10^4 K is comparable with that for PVAc (2.7×10^4 K).[12] The low value of x, 0.11, indicates a very strong dependence of the relaxation time on structure. The β parameter is also low, corresponding to a very broad $g(\tau)$ and is consistent with the broad dielectric loss peaks for PVC near T_g[14] (width at half-height of ca. 5.0 decades, corresponding to a β of ca. 0.25). This may reflect the

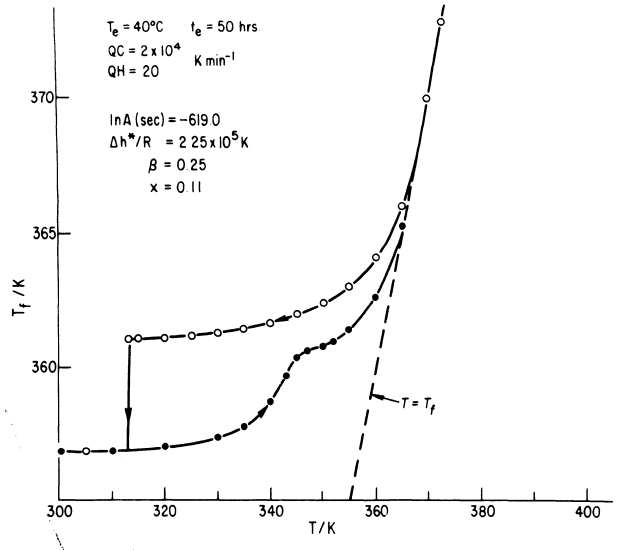

Figure 13. Calculated variation of T_f with T during cooling, annealing, and reheating. Curves correspond to calculated C_p behavior shown in Figure 12C for t_e = 50 h at 40 °C.

presence of ordered regions since the chain segments within the amorphous phase adjacent to the immobile ordered regions would be expected to have a reduced configurational mobility and correspondingly longer relaxation times. This tentative interpretation is supported by data for PVAc (β = 0.51)[12] and preliminary data for polystyrene ($\beta \simeq 0.6$)[29] (both polymers are completely amorphous).

6. Effects of Nonexponentiality. When $\beta = 1$ the relaxation is exponential (single relaxation time) and no sub-T_g endothermic peak is observed (Figure 2). No combination of model parameters and experimental parameters, including those which enhance peak development (e.g., low x, high Q_C, and very long t_e), was found which would generate a sub-T_g endotherm when $\beta = 1$. The pronounced exotherm and endotherm near T_g calculated for $\beta = 1$ (Figure 2) are a direct result of the change in glass transition kinetics and occur identically in unannealed glasses in which the cooling rate was decreased to produce the same T_f as the annealed glass. Thus, for an exponentially relaxing system the C_p behavior during reheating depends only on the starting value of T_f and is independent of how that T_f was achieved. The experimentally observed dependence of C_p behavior on prior history is another example of the well-established fact that memory effects in glasses are a direct reflection of nonexponentiality.

The sub-T_g heat capacity peaks correspond to a rapid increase in enthalpy, followed by a leveling off (or a decrease when an exothermic minimum in C_p is observed). This is illustrated in Figure 13, which shows the calculated temperature dependence of T_f during cooling, annealing, and reheating. The model parameters, cooling rate, and heating rate are those for the PVC fit shown in Figure 13 for an annealing time of 50 h at 40 °C. The reheating curve is similar to the time dependence of volume following two temperature jumps of opposite sign separated by a holding time, first observed by Kovacs.[4] In a qualitative sense the cooling may be equated with a step decrease in temperature, annealing time equated with the holding time, and heating equated with the second temperature jump. More accurately, the response to a cooling–annealing–reheating cycle is the superposition of responses to many of these temperature jump sequences with different holding times.

7. Effect of Nonlinearity. When $x = 1.0$ (linear relaxation) the development of sub-T_g endotherms is completely suppressed for practicable observation times (Figure 3). Calculations indicate that when $x = 1$, production of an observable sub-T_g endotherm, after annealing at 40 °C, for example, is not eliminated but would require annealing times of the order of 10^2–10^3 years. The importance of nonlinearity in accelerating the rate of development of sub-T_g peaks with annealing is readily explained. The glassy state before annealing is characterized by T_f being much higher than T (indeed, the frozen-in value of T_f is one measure of T_g). For increasingly nonlinear systems in which the average relaxation time has a greater dependence on T_f, relaxation will be faster and ΔT_f will be greater. This occurs even though the frozen-in value of T_f for more nonlinear systems is somewhat lower (for the same reason). The increase in ΔT_f enhances the magnitude and rate of development of sub-T_g peaks on reheating in the same way that increased quench rates and longer annealing times do. In addition, increasingly nonlinear systems are more self-accelerating during reheating, which also contributes to the increase in $C_{p\,max}$.

It is of further interest to compare, briefly, the effects of nonexponentiality and nonlinearity on the development of sub-T_g endotherms with annealing with their effects on overshoot behavior near T_g during heating of unannealed glasses. Both phenomena are enhanced by nonlinearity because a nonlinear relaxation is self-accelerating during heating. However, although increasing nonexponentiality enhances the development of endotherms with annealing, it decreases the overshoot at T_g for rate-cooled glasses.[10] The latter is a direct reflection of the approach to equilibrium near T_g being spread over a large temperature range.

VI. Summary and Conclusions

The occurrence of sub-T_g endothermic heat capacity maxima observed in DSC scans of annealed polymeric glasses is a relaxation effect due to the superposition of nonlinear and nonexponential responses to previous thermal history. A simple adaptation of the successful treatment of the glass transition kinetics of Moynihan and co-workers,[5,10-12] reproduces the following experimental observations:

1. The sub-T_g peaks are asymmetric, with long low-temperature tails and relatively steep high-temperature edges.

2. The peaks increase in magnitude ($C_{p\,max}$) and shift to higher temperatures (T_{max}) with increased annealing time (t_e) and annealing temperature (T_e). At long t_e and/or high T_e, the sub-T_g peaks merge with the glass transition and become the well-known C_p overshoot.[15,17-20]

3. The decrease in enthalpy after annealing, ΔH (measured in the model by the decrease in T_f, ΔT_f), is proportional to T_e if $T_g - T_e \geq 20$ K.[15,16,18-20] As T_e approaches T_g, ΔT_f begins to decrease with increasing T_e.[16,20] Similar behavior is exhibited by $C_{p\,max}$.

4. ΔH and $C_{p\,max}$ are approximately linear functions of log t_e. This is reported explicitly,[3,15,17,19] and is also found from plotting data contained in other papers.[16,18]

5. T_{max} is an approximately linear function of T_e. This, too, has been reported explicitly[3,15] and is implicit in other data.[16,18]

6. T_{max} is an approximately linear function of log t_e. Again, this is reported explicitly[3,15] and implicitly.[16,17,19,22]

7. The rate of development of the C_p peaks with annealing increases with increasing quench rate before annealing.

8. Increased heating rate increases T_{max} and increases $C_{p\,max}$.[3,19,25] T_{max} is an approximately linear function of log Q_H.

Acknowledgment. This work was supported in part by National Science Foundation Grant No. CPE-7920740 under the Industry–University Cooperative Research Program. It is a pleasure to acknowledge the programming assistance of R. Iden and useful discussions with Professor H. B. Hopfenberg. We thank the BFGoodrich Co. for permission to publish.

References and Notes

(1) Struik, L. C. E. "Physical Aging in Amorphous Polymers and Other Materials"; Elsevier: Amsterdam, 1978.
(2) Kovacs, A. J.; Aklonis, J. J.; Hutchinson, J. M.; Ramos, A. R. *J. Polym. Sci., Polym. Phys. Ed.* **1979**, *17*, 1097.
(3) Kovacs, A. J. *Fortschr. Hochpolym. Forsch.* **1963**, *3*, 394.
(4) Hodge, I. M.; Berens, A. R. *Macromolecules* **1981**, *14*, 1598.
(5) Moynihan, C. T.; Macedo, P. B.; Montrose, C. J.; Gupta, P. K.; DeBolt, M. A.; Dill, J. F.; Dom, B. E.; Drake, P. W.; Easteal, A. J.; Elterman, P. B.; Moeller, R. P.; Sasabe, H.; Wilder, J. A. *Ann. N.Y. Acad. Sci.* **1976**, *279*, 15.
(6) Lindsey, C. P.; Patterson, G. D. *J. Chem. Phys.* **1980**, *73*, 3348.
(7) Tool, A. Q. *J. Am. Ceram. Soc.* **1946**, *29*, 240.
(8) Gardon, R.; Narayanaswamy, O. S. *J. Am. Ceram. Soc.* **1970**, *53*, 148.
(9) Narayanaswamy, O. S. *J. Am. Ceram. Soc.* **1971**, *54*, 691.
(10) Debolt, M. A.; Easteal, A. J.; Macedo, P. B.; Moynihan, C. T. *J. Am. Ceram. Soc.* **1976**, *59*, 16.
(11) Moynihan, C. T.; Easteal, A. J.; Tran, D. C.; Wilder, J. A.; Donovan, E. P. *J. Am. Ceram. Soc.* **1976**, *59*, 137.
(12) Sasabe, H.; Moynihan, C. T. *J. Polym. Sci.* **1978**, *16*, 1447.
(13) Berens, A. R.; Hodge, I. M. *Macromolecules*, preceding paper in this issue.
(14) McCrum, N. G.; Read, B. E.; Williams, G. "Inelastic and Dielectric Effects in Polymeric Solids"; Wiley: New York, 1967.
(15) Illers, K. H. *Makromol. Chem.* **1969**, *127*, 1.
(16) Foltz, C. R.; McKinney, P. V. *J. Appl. Polym. Sci.* **1969**, *13*, 2235.
(17) Weitz, A.; Wunderlich, B. *J. Polym. Sci.* **1974**, *12*, 2473.
(18) Wyzgoski, M. G. *J. Appl. Polym. Sci.* **1980**, *25*, 1455.
(19) Petrie, S. E. B. *J. Polym. Sci., Part A-2* **1972**, *10*, 1255.
(20) Gray, A.; Gilbert, M. *Polymer* **1976**, *17*, 44.
(21) Straff, R.; Uhlmann, D. *J. Polym. Sci., Polym. Phys. Ed.* **1976**, *14*, 1087.
(22) Shultz, A. R.; Young, A. L. *Macromolecules* **1980**, *13*, 663.
(23) O'Reilly, J. M. *J. Appl. Phys.* **1979**, *50*, 6083.
(24) Robertson, R. E. *J. Appl. Phys.* **1978**, *49*, 5048.
(25) Prest, W. M., Jr.; O'Reilly, J. M.; Roberts, F. J., Jr.; Mosher, R. A. *Polym. Eng. Sci.* **1981**, *21*, 1181.
(26) Brown, I. G.; Wetton, R. E.; Richardson, M. J.; Savill, N. G. *Polymer* **1978**, *19*, 659.
(27) Prest, W. M., Jr.; Roberts, F. J., Jr. *Ann. N.Y. Acad. Sci.* **1981**, *371*, 67.
(28) Moynihan, C. T.; Easteal, A. J.; Wilder, J.; Tucker, J. *J. Phys. Chem.* **1974**, *78*, 2673.
(29) Hodge, I. M., unpublished data.